

# CALCULATION OF A RELATIVISTIC 300 GHz RANGE GYROTRON, CONSIDERING THE REAL SHAPE OF THE ACCELERATING VOLTAGE PULSE

© 2025 A. N. Leontyev\*, R. M. Rozental, O. P. Plankin, E. S. Semenov

*Federal Research Center A.V. Gaponov-Grekhov Institute of Applied Physics of the  
Russian Academy of Sciences, Russia*

\*e-mail: [leontiev@ipfran.ru](mailto:leontiev@ipfran.ru)

Received September 06, 2024

Revised September 16, 2024

Accepted September 30, 2024

**Abstract.** Calculations have been performed for a relativistic gyrotron in the 300 GHz range with a power of up to 8 MW. For the experimentally measured accelerating voltage pulse shape, calculations of the output power pulse shape were made using three-dimensional modeling using the large particle method. It has been shown that the total radiation energy at the operating frequency can exceed 4 J.

**Keywords:** *relativistic gyrotron, terahertz radiation*

**DOI:** [10.31857/S03676765250123e5](https://doi.org/10.31857/S03676765250123e5)

## INTRODUCTION

Powerful pulsed terahertz radiation is of interest for many applications. In turn, such radiation can be produced on the basis of one or another scheme of vacuum generators with electron fluxes. In particular, the project of generating radiation of subgigawatt power level in the range of 0.3-1 THz based on free electron lasers is being intensively developed at present [1-4]. It is estimated that the energy of the generated radiation pulses will be in the range of 10-100 J. Comparable power levels can also be

obtained using relativistic gyrotrons. Thus, in [5] it was shown that on the basis of high-current relativistic electron fluxes the power of the order of 80 MW in the range of 0.3 THz can be achieved. However, high-current electron fluxes, usually formed by explosive emission cathodes, have a significant disadvantage related to the short duration of pulses. In this connection, it is of interest to use thermionic emission cathodes capable of forming electron fluxes with stable parameters with microsecond duration. In [6], calculations of the electron-optical system of a relativistic gyrotron of the 300 GHz range based on a magnetron- injection gun with a thermocathode were performed. It was shown that for the specified frequency range it is possible to form a helical electron flux with a current of 100 and more amperes, an energy of 250 keV, and a pitch factor value of 1.1.

At the new stage of research, calculations of the electron-wave interaction of the gyrotron with the working mode  $TE_{33,2}$ .

## AVERAGED EQUATION MODELING

In the development of long-pulse terahertz gyrotrons, the main task is to solve the problem of mode competition. In this regard, it is attractive to use whispering gallery modes whose fields are localized near the resonator walls [7]. As a consequence, when the electron flow is transported near the resonator wall, the self-excitation conditions will be fulfilled only for the whispering gallery modes. However, during experimental studies, it became clear that selective excitation of modes of the  $TE_{(m),1}$  type already at the value of the number of azimuthal variations  $m \geq 9$  is possible only by using additional selection methods, for example, by introducing a coaxial metal

rod into the resonator [8,9]. In turn, for modes of the  $TE_{(m)(,2)}$  type, the situation is much better. In particular, a 303 GHz gyrotron has been successfully realized on the  $TE_{22,2}$  mode [10]. At the same time, there is an upper limit to the azimuthal index of the working mode. In [11], estimates were made that stable generation on whispering gallery modes can be realized quite easily at azimuthal index values  $m \leq 30$ . Estimates show, that for the studied configuration of the gyrotron the optimal value for the azimuthal index  $m = 33$ , which corresponds to the working mode  $TE_{33,2}$ . This is due to the need to ensure the maximum of the electron-wave interaction coefficient. This coefficient is determined by the radius of the electron flux encounter, which, in turn, is determined by the configuration of the electron-optical system. The radius of the homogeneous section of the resonator was chosen to be 6.65 mm, which corresponds to the critical frequency value of about 300.7 GHz. Optimization of the resonator geometry was carried out on the basis of calculations of the electron-wave interaction in the framework of the stationary single-mode gyrotron equations with an unfixed field structure.

In the framework of this approach, the normalized complex transverse momentum  $p_c$  of each electron when moving along the longitudinal axis  $z \in [z_{in}, z_{out}]$  is described by the equation

$$\begin{aligned}
 \frac{dp_c}{dz} + i \frac{p_c}{p_{\parallel}} \left( \frac{\gamma \kappa}{n} - \frac{\omega_{Ho}}{c} \right) = \kappa_{\perp} \frac{\mathcal{J}_{m,p,n}}{\mathcal{N}_{m,p}} \cdot \left\{ \left( \frac{i \gamma F}{p_{\parallel}} + \frac{1}{\kappa} \frac{dF}{dz} \right) \cdot (p_c^*)^{n-1} \cdot \mathcal{B}_- + \right. \\
 \left. + \left( \frac{i \gamma F^*}{p_{\parallel}} - \frac{1}{\kappa} \frac{dF^*}{dz} \right) \cdot p_c^{n+1} \cdot \mathcal{B}_+ - i p_c \cdot \text{Re} \left( \frac{F}{p_{\parallel}} \cdot (p_c^*)^n \right) \cdot \frac{\kappa_{\perp}}{\kappa} \cdot \mathcal{B}_0 \right\} \\
 + p_c \cdot \mathcal{M}' \tag{1}
 \end{aligned}$$

where  $\gamma$  is the relativistic mass-factor,  $n$  is the number of the cyclotron harmonic,  $c$  is the speed of light,  $\mathcal{J}_{m,p,n}(r, z) = s^n \cdot J_{s \cdot (m-n)} \left( v_{m,p} \cdot \frac{r}{R_r(z)} \right)$  is the coupling factor of the  $\text{TE}_{m,p}$  mode with the electron beam with the radius of the leading centers  $r$  at the  $n$ -th harmonic,  $\mathcal{N}_{m,p}^2 = (v_{m,p}^2 - m^2) \cdot J_m^2(v_{m,p})$  is the norm of the  $\text{TE}_{m,p}$  wave, where  $s = +1$  for  $m \geq 0$  or  $s = -1$  for  $m < 0$ , i.e., in the case of the opposite rotation of the field relative to the Larmor rotation of the electrons, i.e., in the case of opposite field rotation with respect to the Larmor rotation of the electrons.  $\mathcal{B}_- = \frac{J_{n-1}(\xi)}{2p_{\perp}^{n-1}}$ ,  $\mathcal{B}_+ = \frac{J_{n+1}(\xi)}{2p_{\perp}^{n+1}}$ ,  $\mathcal{B}_0 = \frac{J_n(\xi)}{p_{\perp}^n}$ ,  $\mathcal{B}_1 = \frac{J'_n(\xi)}{p_{\perp}^{n-1}}$  - force interaction coefficients.  $J'_l \equiv dJ_l(\xi)/d\xi$ ,  $\xi = \kappa_{\perp} \cdot r_L r_L = p_{\perp} \cdot c / \omega_{Ho}$  is the Larmor radius of the electron orbit,  $p_{\perp}^2 = p_c \cdot p_c^* \mathcal{M}'(z) \equiv \frac{1}{2\mathcal{M}(z)} \cdot \frac{d\mathcal{M}}{dz}$ . - normalized derivative of the magnetic field. In the case of a homogeneous magnetic field it is assumed  $\mathcal{M} = 1$ ,  $\mathcal{M}' = 0 \ \forall z$

The nonrelativistic circular gyrofrequency (Larmor, cyclotron frequency) of the electron is proportional to the magnetic field at any point of its trajectory:  $\omega_{Ho} = \mathcal{M}(z) \cdot B_0 \cdot e_0 / m_0$ , where  $e_0$  and  $m_0$  are the charge (modulo) and rest mass of the electron.

The longitudinal component of the normalized momentum  $p_{\parallel}$  is described by Eq:

$$\frac{dp_{\parallel}}{dz} = -Re \left( \frac{1}{\kappa} \frac{dF}{dz} \cdot (p_c^*)^n \right) \cdot \mathcal{B}_1 \cdot \frac{\kappa_{\perp}}{p_{\parallel}} \cdot \frac{\mathcal{J}_{m,p,n}}{\mathcal{N}_{m,p}} - \frac{p_{\perp}^2}{p_{\parallel}} \cdot \mathcal{M}' \quad (2)$$

where the last summand describes the influence of inhomogeneous static magnetic field.

The equation describing the longitudinal structure of the high-frequency field amplitude  $F$ , has the form [12]:

$$\frac{d^2F}{dz^2} + \kappa_{\parallel}^2 F = \frac{I}{\mathcal{N}_{m,p}} \cdot \kappa \cdot \kappa_{\perp} \cdot \langle \langle \mathcal{J}_{m,p,n} \cdot \frac{p_c^n}{p_{\parallel}} \cdot \mathcal{B}_1 \rangle \rangle. \quad (3)$$

Initial pulse values for different electron beam fractions:

$$p_c(z_{in}) = p_{c,in}, \quad p_{\parallel}(z_{in}) = p_{\parallel,in} \quad (4)$$

are determined based on the given values of voltage  $U_0$ , pitch factor  $g$  and taking into account the inhomogeneity of the magnetic field.

The complex field amplitude  $F(z)$  satisfies the radiation boundary conditions at the ends of the integration interval : $z \in [z_{in}, z_{out}]$

$$\frac{dF(z)}{dz} = i \kappa_{\parallel} F(z) \text{ at } z = z_{in}; \quad (5)$$

$$\frac{dF(z)}{dz} = -i \kappa_{\parallel} F(z) \text{ at } z = z_{out}. \quad (6)$$

The profile of the resonator and adjacent waveguide transitions  $R_r(z)$  must be sufficiently smooth: the limiting angles  $\alpha$  of the slope of the waveguide side-surface pattern must at least satisfy the condition  $\operatorname{tg} \alpha \ll 1$ . The wave number  $\kappa = \omega c$  is one of the eigennumbers of the problem along with  $F_{in}$ . Let us write down the longitudinal wave number  $\kappa_{\parallel}$  taking into account ohmic losses in the following form

$$\kappa_{\parallel}^2(z) = \kappa^2 - \kappa_{\perp}^2(z) \cdot \Omega(z), \quad (7)$$

where  $\kappa_{\perp}(z) = v_{m,p}/R_r(z)$  is the transverse wave number at a given cross section , $z$  is the speed of light,  $v_{m,p}$  is  $p$  the root of the derivative of the Bessel function  $J_m$

Complex multiplier

$$\Omega(z) = 1 + \frac{i}{Q_{ohm}} \cdot \frac{R_{reg}}{R_r(z)} \quad (8)$$

allows one to take into account the energy losses for heating of the resonator. Here  $R_{reg}$  is the radius of the homogeneous section of the resonator,

$$Q_{\text{ohm}} = \left(1 - \frac{m^2}{v_{m,p}^2}\right) \cdot \frac{R_{\text{reg}}}{\delta_{\text{skin}}}, \quad (9)$$

-- ohmic goodness of fit,  $\delta_{\text{skin}} = k_{\text{skin}} \cdot \delta_{\text{idl}}$  - skin layer thickness,  $\delta_{\text{idl}} = \sqrt{2/(Z_0 \sigma \mu_r \omega)}$  - skin layer thickness of smooth metal (without roughness),  $Z_0 = \sqrt{\mu_0 / \epsilon_0} \approx 376.73$  Ohm - vacuum wave impedance,  $\mu_r \approx 1$  - relative magnetic permeability of metal,  $\sigma$  - its temperature-dependent specific DC conductivity (inverse resistance);  $k_{\text{skin}} \approx 1.5 - 3$  - loss coefficient, which takes into account the influence of microroughnesses on the resonator surface [13]; in general, this coefficient depends on frequency and temperature.

Fig. 1 shows the optimized resonator profile, the length of the homogeneous section of the resonator is about 10 mm. The maximum generation power in the resonator with this profile is achieved at a magnetic field of 14.7 Tesla and is 8 MW, which corresponds to an efficiency of about 32%.

### THREE-DIMENSIONAL MODELING BY LARGE PARTICLE METHOD

Modeling of processes at the front of the accelerating voltage pulse was carried out on the basis of the three-dimensional PIC code KARAT [14]. Fig. 2 shows the geometry of the interaction space and the instantaneous position of macroparticles. From the left boundary, a helical electron beam was injected into the system with a pitch factor of 1.1 and a magnitude of the initial spread in transverse velocities of about 30%. The magnetic field was set constant over a homogeneous section of the resonator. Further, a gradual decrease in the magnitude of the longitudinal component of the magnetic field was set, as a result of which the electron beam was deposited on the

wall of the electrodynamic system. On the right boundary of the system, an absorbing layer with variable conductivity was set, the reflection coefficient from which did not exceed 1% in power. The electrical conductivity of the walls was set equal to the electrical conductivity of copper.

Fig. 3 shows the experimentally measured oscillogram of the time dependence of the accelerating voltage. It can be seen that the presented pulse contains a rising edge with a duration of about 1  $\mu$ s. However, at the moment, three-dimensional PIC modeling of gyrotron dynamics at such times would take a very large amount of real time. In order to reduce the computational time, the shape of the accelerating voltage pulse, close in shape to the experimentally measured one, but with a total duration of about 350 ns, was used in the simulation.

The duration of the accelerating voltage edge was about 150 ns. Such a reduction in the front duration should not lead to a significant change in the dynamics of the system, since the front duration significantly exceeds the characteristic times of oscillation establishment  $\sim Q/(2\pi f)$ , where  $Q$  and  $f$  are the goodness of fit and natural frequency of the mode.

Due to some limitations of the KARAT code, only discrete changes of the initial particle pitch factor with the number of values not exceeding four could be specified in the simulation. As a consequence, we used the following algorithm for modeling the turn-on scenario: the electron beam was represented as a sequence of four electron pulses with durations of 20, 40, 40, and 60 ns. The transition between pulses was realized by decreasing to zero the current and electron energy at the trailing edge of the pulse and simultaneously increasing from zero to the required value of the current and

electron energy at the leading edge of the next pulse. During each of the pulses, the pitch factor remained constant. Its value was set equal to the average value of the pitch factor at a given time interval, calculated on the basis of the calculation of the electron-optical system. The size of the counting grid in the simulation was set equal to  $175 \times 175 \times 231$  nodes, the number of macroparticles was about 100000.

The modeling showed that selective excitation of oscillations on the TE33.2 mode occurs in the range of magnetic fields from 14.6 to 15.1 Tesla. The maximum generation power was about 7 MW, which is very close to the value calculated on the basis of the averaged equations. The difference between the generation frequency obtained in the PIC modeling and the generation frequency calculated based on the averaged equations is less than 2%. This is an acceptable value considering the used dimensionality of the counting grid.

Modeling showed that in the optimal generation mode the total duration of oscillation generation on the working mode in the 300 GHz range is about 100 ns (Fig. 3), which corresponds to about 600 ns of time in a real system. Thus, taking into account the maximum generation power of about 7 MW, the total energy of the pulsed terahertz radiation can exceed 4 J.

## CONCLUSION

Gyrotrons based on relativistic helical electron fluxes appear to be promising sources of powerful terahertz radiation. First of all, it should be noted the relatively high efficiency of electron-wave interaction in comparison with other types of sources. Confirmations of the possibility of creating highly efficient relativistic gyrotrons were

obtained in previous experimental studies. In particular, in the Ka-band gyrotron, radiation with a microsecond pulse duration with a power of about 10 MW and an efficiency of about 50% was obtained [15], and in the W-band gyrotron, radiation with a duration of about 0.5  $\mu$ s with a power of more than 5 MW and an efficiency of about 20% was obtained [16]

The presented work demonstrates that it is possible to further increase the operating frequency of the relativistic gyrotron up to the terahertz range while maintaining the efficiency of electron-wave interaction at the level of 30%. It is important to note that the required values of the leading magnetic field (about 15 Tesla) are currently achievable not only in pulsed solenoids but also in cryomagnets. Taking into account the possibility of operation of high-voltage power supplies with a high frequency of repetition, this opens up prospects for the use of such sources in a number of plasma applications [17,18].

## FUNDING

The research was carried out within the framework of the topic of the state assignment FFUF-2022-0007.

## REFERENCES

1. *Peskov N.Yu., Zaslavsky V.Yu., Ginzburg N.S. et al. // Radiophys. Quantum Electron.* 2023. V. 66. No. 7-8. P. 513.
2. *Sandalov E.S., Sinitsky S.L., Arzhannikov A.V. et al. // Radiophys. Quantum Electron.* 2023. V. 66. No. 7-8. P. 489.
3. *Peskov N.Yu., Arzhannikov A.V., Belousov V.I. et al. // Bull. Russ. Acad. Sci.* 2023.

V. 87. No. 5. P. 669.

4. *Sandalov E.S., Sinitsky S.L., Arzhannikov A.V. et al.* // Bull. Russ. Acad. Sci. 2023.

V. 87. No. 5. P. 573.

5. *Rozental R.M., Danilov Y.Y., Leontyev A.N., et al. et al.* // IEEE Trans. Electr. Dev.

2022. V. 69. No. 3. P. 1451.

6. *Danilov Yu.Yu., Leontyev A.N., Plankin O.P. et al.* // Bull. Russ. Acad. Sci. Phys.

2024. V. 88. No. 1. P. 80.

7. *Vainshtein L.A.* Open resonators and open waveguides. Golem Press, 1969.

8. *Bykov Y.V., Gol'denberg A.L., Nikolaev L.V. et al.* // Radiophys. Quantum Electron.

1975. V. 18. P. 1141.

9. *Gaponov A.V., Flyagin V.A., Goldenberg A.L. et al.* // Int. J. Electron. 1981. V. 51.

No. 4. P. 277.

10. *Saito T., Tanaka S., Shinbayashi R. et al.* // Plasma Fusion Res. 2019. V. 14. Art.

No. 1406104.

11. *Nusinovich G.S.* // IEEE Trans. Plasma Sci. 1999. V. 27. No. 2. P. 313.

12. *Zavolskiy N.A., Zapevalov V.E., Moiseev M.A.* // Izv. of Vuzov. Radiophys. 2001.

T. 44. № 4. C. 345.

13. *Zapevalov V.E., Zuev A.S., Parshin V.V. et al.* // Izv. of universities. Radiophys.

2021. T. 64. № 4. C. 265.

14. *Tarakanov V.P.* // EPJ Web Conf. 2017. V. 149. Art. No. 04024.

15. *Zaitsev N.I., Zavolskiy N.A., Zapevalov V.E. et al.* // Izv. of universities. Radiophys.

2003. T. 46. № 10. C. 914.

16. *Abubakirov E.B., Chirkov A.V., Denisov G.G. et al.* // IEEE Trans. Electron Dev.

2017. V. 64. No. 4. P. 1865.

17. *Sidorov A.V., Veselov A.P., Vodopyanov A.V. et al.* // Tech. Phys. Lett. 2023. V. 49.

No. 12. P. 77.

18. *Vodopyanov A.V., Glyavin M.Y., Golubev S.V., et al.* // Letters in ZhTF. 2017. T. 43.

№ 4. C. 10.

#### FIGURE CAPTIONS

**Fig. 1.** Results of calculations using the averaged equations: the optimal resonator profile and the dependence of efficiency on the longitudinal coordinate.

**Fig. 2.** Geometry of the interaction space and instantaneous position of macroparticles in the longitudinal and cross sections of the system.

**Fig. 3.** Experimental oscillogram of accelerating voltage (a), time scale of one cell is 500 ns; dependence of electron energy (b) and output power (c) in the optimal mode in three-dimensional modeling by the large-particle method.

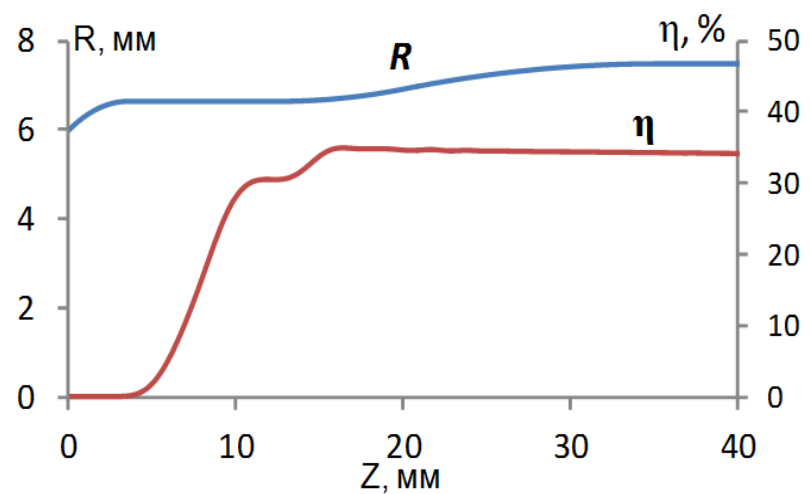


Fig. 1.

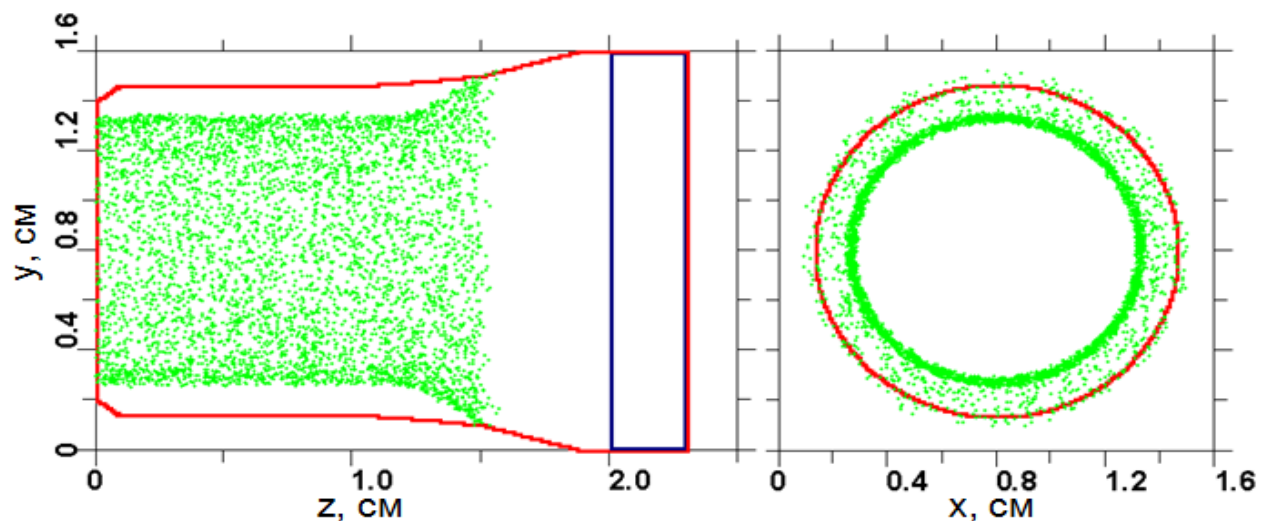


Fig. 2

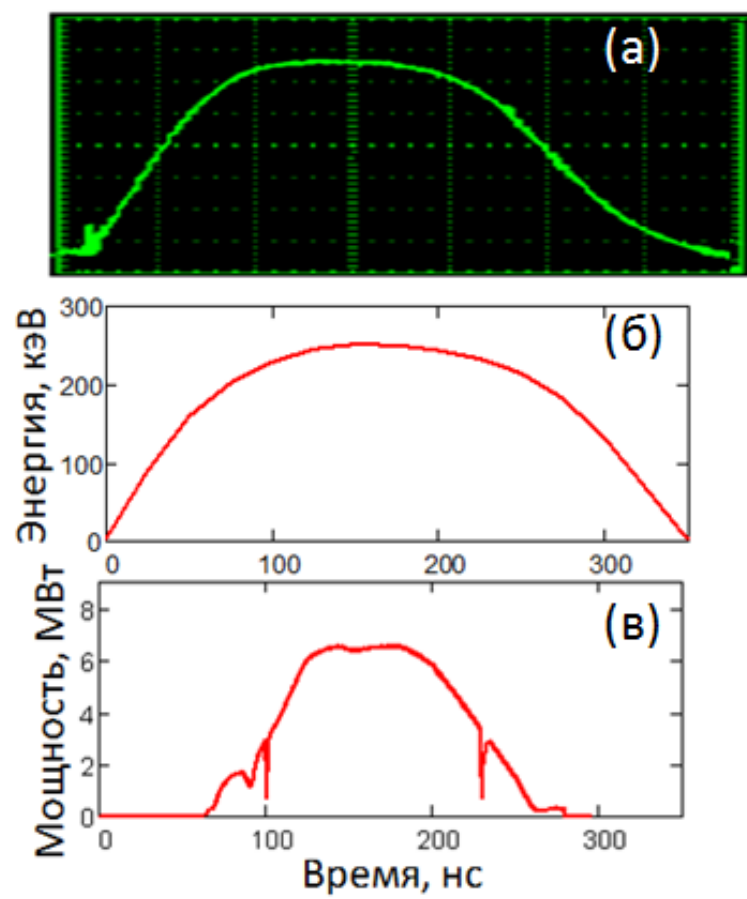


Fig. 3.